



Calhoun: The NPS Institutional Archive
DSpace Repository

Faculty and Researchers

Faculty and Researchers' Publications

1973-07-01

Charge depletion mechanism operative in space-charge flows

Biblarz, O.; Bohley, C.M.

American Institute of Physics

Journal Name: J. Appl. Phys.; (United States); Journal Volume: 44:7
<https://hdl.handle.net/10945/60971>

This publication is a work of the U.S. Government as defined in Title 17, United States Code, Section 101. Copyright protection is not available for this work in the United States.

Downloaded from NPS Archive: Calhoun



Calhoun is the Naval Postgraduate School's public access digital repository for research materials and institutional publications created by the NPS community. Calhoun is named for Professor of Mathematics Guy K. Calhoun, NPS's first appointed -- and published -- scholarly author.

Dudley Knox Library / Naval Postgraduate School
411 Dyer Road / 1 University Circle
Monterey, California USA 93943

<http://www.nps.edu/library>

Charge depletion mechanism operative in space-charge flows

Oscar Biblarz and Carl M. Bohley*

Naval Postgraduate School, Monterey, California 93940
(Received 5 February 1973)

Charge depletion is considered for negatively charged particles flowing with a dielectric medium (air). The problem is representative of those encountered in electrodynamic devices. A mechanism is proposed wherein electrons are depleted from the particles by the formation of O_2^- . These ions, being some 100 times more mobile than the particles, are essentially lost from the flow because of their high slip. Axisymmetric jets mixing with ambient air are investigated, and a computer program is used to solve the combined Poisson/Laplace equations. Results ranging from no-charge depletion to total depletion are presented.

I. INTRODUCTION

A basic ingredient in electrodynamic (EGD) generators is the convection of charged particles against an electric field. Typically, these particles are negatively charged and, because their size is in the micron range, each can have many electrons. For example, the Rayleigh or stability limit for a micron-size water droplet is about 6×10^4 electrons. Charging may range from a single electron per particle to the Rayleigh limit; the actual particle size and charge are optimized^{1,2} for each individual application. In this paper, water droplets in air at standard conditions will be considered.

The question arises as to what charge depletion mechanisms are operative in such a space-charge flow. If wall effects are discarded, the choice is narrowed down considerably. Electron emission^{3,4} from the droplet can be ruled out in a straightforward way; the fields that the dielectric fluid may withstand are just too small for substantial electron emission and the droplet temperature is, of course, too low for thermionic emission. Charge break up or coalescence may be significant (as it is in thunder clouds⁵) but only if the particles are originally charged to the Rayleigh limit. Droplet stability is very difficult to discuss in general⁶ and it will be assumed that the droplets are stable (in EGD, solid particles may be used, in which case size stability is assured).

One important mechanism for charge depletion that appears to be overlooked^{7,8} is the formation of negative ions. Even though free electrons have the highest mobility in an electric field, ion mobilities are also high compared to those of the particulates. This is the very reason why molecular ions are not used in EGD. In fact, unless the charged particles have a mobility less than 100 times that of the ions, they will not couple the electric field to the flow field efficiently.⁹ If the formation of negative ions may occur in substantial numbers at the charged droplet surface, the original space-charge density in the flow may diminish noticeably from the region of charge injection to the region of collection. We shall consider oxygen ions only, because their formation is more probable than those of nitrogen in air at standard conditions.⁴

The proposed depletion mechanism operative in space-charge flows is discussed next. This is followed by solutions to the combined Poisson/Laplace equation for varying degrees of charge depletion in a specific flow configuration.

II. PROPOSED MECHANISM

It will be assumed that the charged particles under consideration are large enough to be describable with continuum concepts. That is, the mean free path of the oxygen molecules is at least a factor of 10 smaller than the diameter of the particle (which restricts this discussion to particles above $1 \mu\text{m}$). In this case, the collision of molecules with a given particle is comparable to the collision of molecules with a wall. If the charged particles have a large excess of electrons, some electrons should be relatively available for attachment with O_2 molecules. Rather than attempting to predict the associated Fermi levels, a value for the attachment probability on an electron with an oxygen molecule at the droplet surface will be assumed. This probability (P_a) should be of the order of 10^{-7} (a value somewhat smaller than those quoted for the capture of a free electron by an O_2 molecule¹⁰). In addition to P_a , a probability denoting the availability of the electron population itself should be included. Clearly, if there are no excess electrons in the droplet, ions would not be anticipated to form. It is expected that the latter probability be given by Z/Z_{max} , where Z denotes the number of electrons per droplet and Z_{max} the Rayleigh limit (which is a function of the droplet radius). Thus, the total probability for ion formation becomes

$$P_a(Z/Z_{\text{max}}).$$

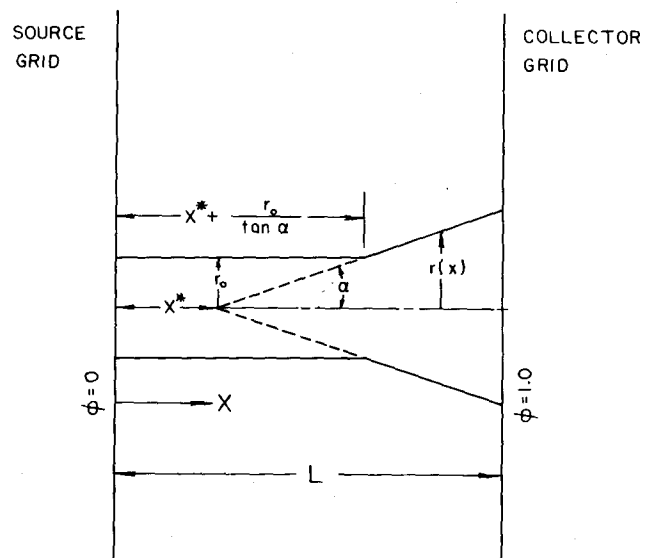


FIG. 1. Geometry of jet.

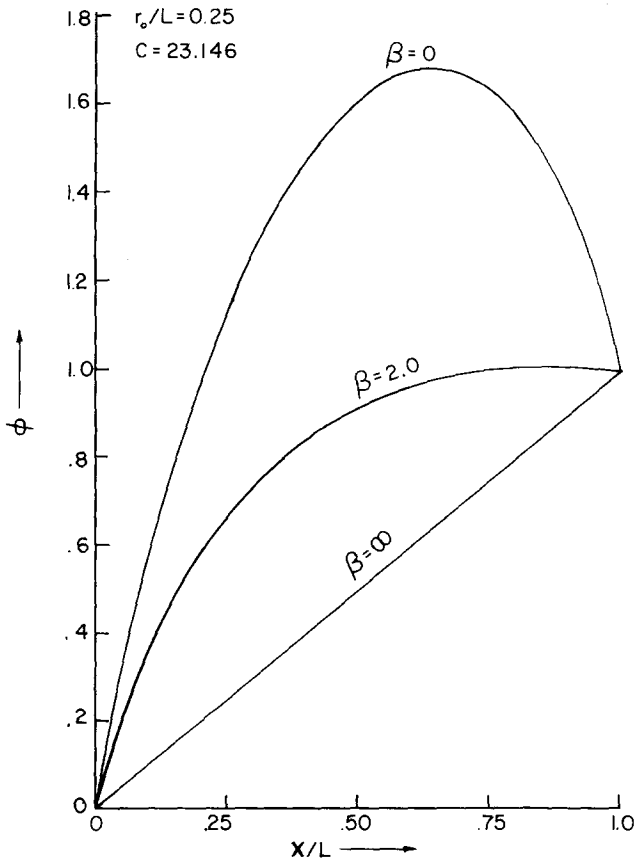


FIG. 2. Centerline potential for straight jet.

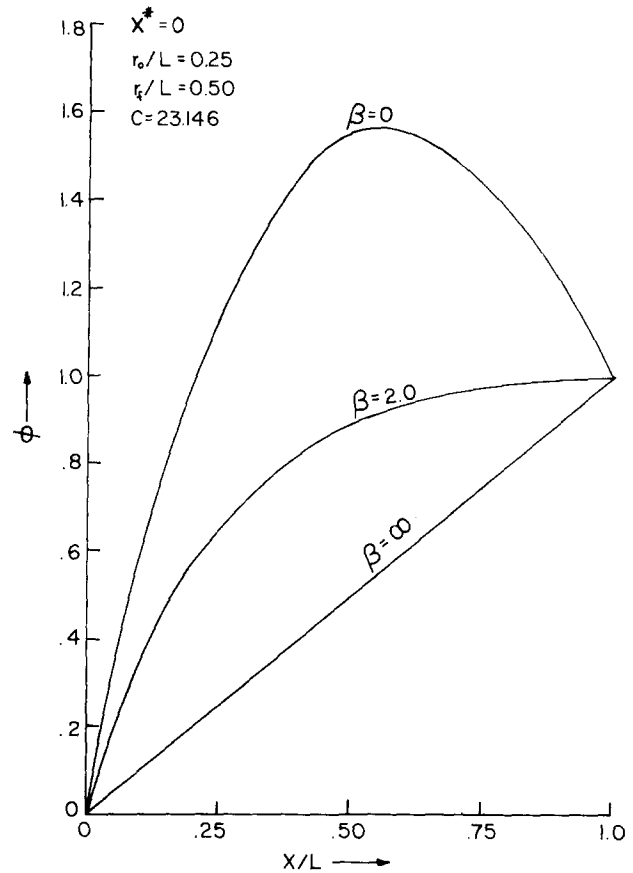


FIG. 3. Centerline potential for expanding jet.

Even though the probability of attachment is low, the collision frequency of the molecules with the droplet is very high at standard conditions (over 10^{15} collisions/sec). The collision frequency will be calculated from $\frac{1}{4}n\bar{c}A_p$, where n is the number density of O_2 , \bar{c} the thermal speed of O_2 , and A_p the area of the particle. Now, the depletion rate for electrons from a particle becomes

$$\frac{dZ}{dt} = - \left(P_a \frac{Z}{Z_{max}} \right) \left(\frac{1}{4}n\bar{c}A_p \right) \tag{1}$$

It is interesting to note that the above equation has the standard form of a recombination equation since it is proportional to the concentrations of two combining species.

The space-charge density is given by

$$\rho = en_p Z,$$

where n_p is the number density of the particles and e is the charge of an electron.

Now, assuming a steady incompressible axisymmetric free jet, the left-hand side of Eq. (1) may be transformed into

$$\frac{dZ}{dt} = v_p \frac{dZ}{dx}, \tag{2}$$

where v_p is the particle velocity in the flow direction and, x is the axial on the flow coordinate. Considering a uniform velocity across the jet, v_p may be written as

$$v_p = v_{p0} \left(\frac{r}{r_0} \right)^2,$$

where v_{p0} is the initial particle (jet) velocity, r_0 the initial jet radius, and $r = r(x)$, the jet radius.

The present model is one where the slip of the particles is negligible so that they move at the jet velocity, whereas the ion slip is so high that upon formation ions essentially disappear upstream of the jet.

Combining Eqs. (1) and (2) and integrating, one gets

$$\ln \left(\frac{Z}{Z_0} \right) = - P_a \frac{n\bar{c}}{4} \frac{A_p}{Z_{max}} \int \frac{dx}{v_p}$$

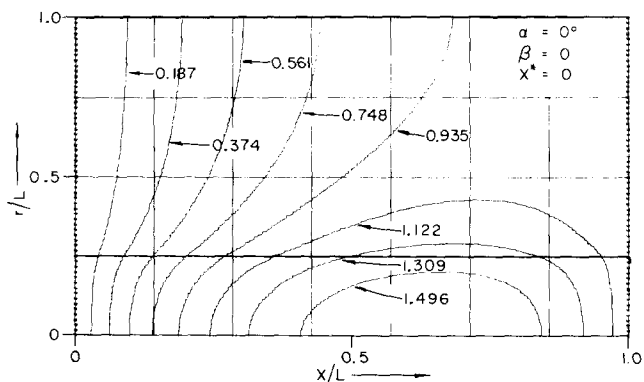


FIG. 4. Potential map ($\alpha = 0, \beta = 0$).

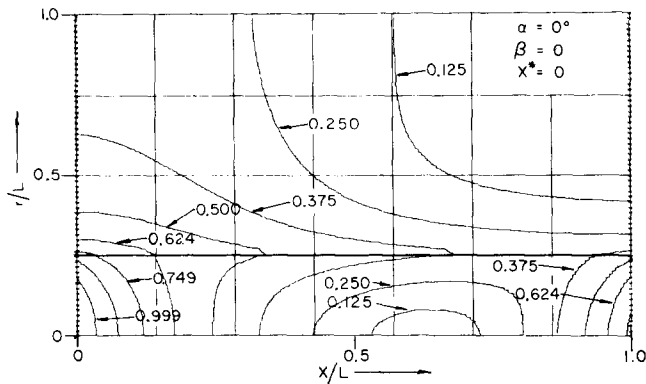


FIG. 5. Electric field map ($\alpha = 0, \beta = 0$).

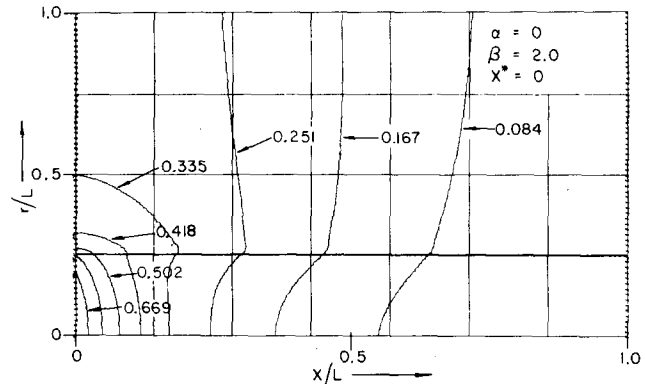


FIG. 7. Electric field map ($\alpha = 0, \beta = 2$).

or

$$\frac{Z}{Z_0} = \exp\left(-\beta \int \frac{d(x/L)}{v_p/v_{p0}}\right), \quad (3)$$

where

$$\beta = P \frac{n\bar{c}}{4} \frac{A_p}{Z_{\max}} \frac{L}{v_{p0}}$$

L is the channel length and Z_0 is the initial charge per particle.

The variation of the jet radius with x remains to be defined.

III. GEOMETRY

For simplicity, a free jet between two infinite parallel grids a distance L apart will be considered. Thus, this case is an extension of the Laplacian solution for the infinite parallel charged plates where now a jet containing space charge is present.

The most common, though not the simplest, jet shape is one where the radius expands due to mixing with the surrounding gas. It turns out that for both laminar and turbulent jets, the growth of the jet boundaries due to mixing is proportional to the axial distance from some virtual origin.¹¹ This is shown in Fig. 1. Even though this description is quite unrestricted, the value of the virtual origin as well as of the expansion angle α can only be given from experiments. Two cases will be treated, namely, a straight jet and one which is of con-

stant radius until $\frac{1}{2}L$, whereupon it grows to twice the radius in a linear fashion. In the latter case, a reduction of the space-charge density due to jet spreading will affect the potential profiles. It should be mentioned here that since a boundary-value problem is being solved, these results will only apply to cases where the domain is similar to ours.

When the jet radius is constant, Eq. (3) becomes

$$Z/Z_0 = \exp(-\beta x/L),$$

and in the expanding section, Eq. (3) becomes

$$\frac{Z}{Z_0} = \exp\left\{-\beta\left[\frac{x^*}{L} + \frac{r_0}{L \tan \alpha} - \frac{1}{3} \frac{r_0^3}{L^3 \tan \alpha} + \frac{1}{3} \frac{(x-x^*)^3}{L^3} \tan^2 \alpha\right]\right\},$$

where x^* is the virtual origin and α is the expansion angle.

Even though the velocity profile of the jet is nonuniform, it will be assumed that the mass-mean-velocity representation is sufficient for the present purposes.

IV. RESULTS

The potential distribution within an EGD device is described by a "combined Laplace-Poisson" equation. The two equations are required by the two-phase space-charge nature of the EGD environment. Poisson's equation models the space-charge region, while Laplace's equation models the space-charge-free region.

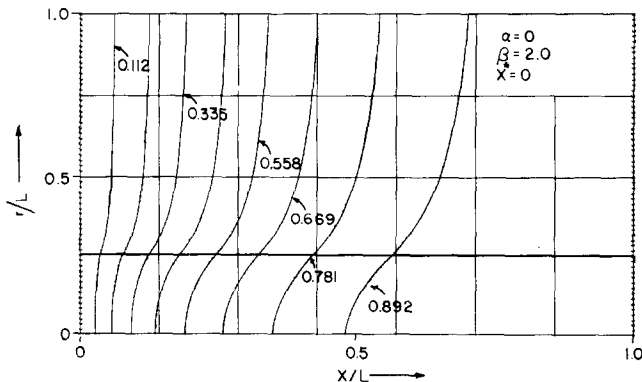


FIG. 6. Potential map ($\alpha = 0, \beta = 2$).

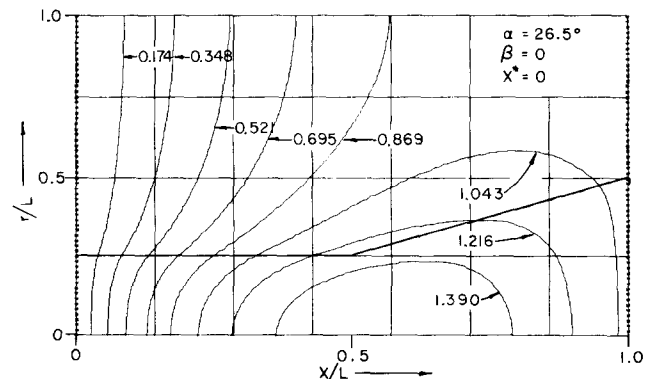


FIG. 8. Potential map ($\alpha = 26.5^\circ, \beta = 0$).

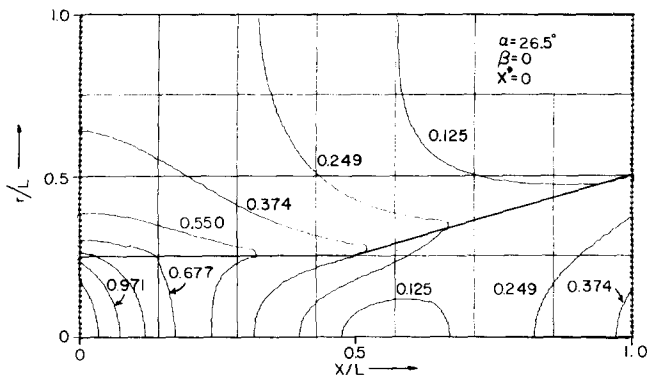


FIG. 9. Electric map ($\alpha = 26.5^\circ, \beta = 0$).

A numerical solution method (successive overrelaxation) for these equations was programmed for the IBM 360 computer system.¹² Finite-difference equations, derived from a Taylor-series expansion about the point in question, were used to build the numerical model. Of importance in the computer modeling of the EGD device is the fluid dynamics involved. By means of a similar program,¹³ it has been shown that for particle sizes of interest, the fluid dynamics may be uncoupled from the electrostatics. Thus, it is possible to limit modeling of the dielectric gas flow to a constant rate of jet expansion and ensure conservation of charge within the jet.

Input variables to the program typically include those describing the electrode geometry, dielectric characteristics, charged-particle characteristics, flow control, variable matrix dimensions, and the output desired. The program generates the jet radius and fills in the space-charge value corresponding to cells within the jet. Outside the space charge is zero but conditions are matched at the boundaries. Similarly, the boundary conditions at the grids are superimposed. The program simulates a steady-state picture of the entire EGD situation by the superposition of two separate matrices. One matrix will carry all potential information, while the other matrix carries both charge distribution and some flow control information. The initial part of the program is devoted to setting up these matrices.

Once the above has been accomplished, the program calls for an iterative calculation to determine the potential distribution and a calculation for the $|E|$ -field distribution. The remainder of the program is devoted to the output of these results.

The nondimensional form of Poisson's equation used is

$$\nabla^2 \phi = C(Z/Z_0),$$

where ϕ is the dimensionless potential, and

$$C = L^2 \rho_0 / \epsilon V_0,$$

where ρ_0 is the initial space-charge density, V_0 the overall or electrode voltage, and ϵ the permittivity of free space.

The following parameters are used in these calculations (the reason is given in Sec. V):

$$r_0/L = 0.25 \text{ and } C = 23.145.$$

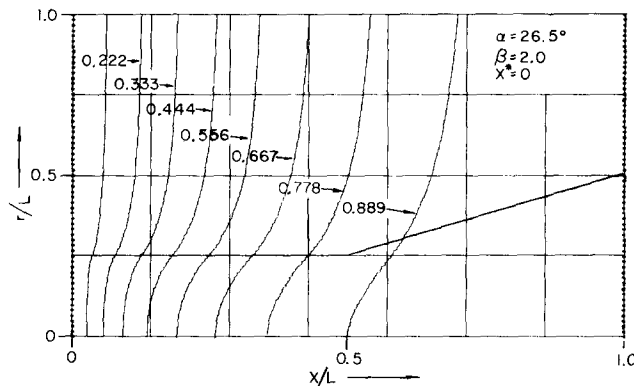


FIG. 10. Potential map ($\alpha = 26.5^\circ, \beta = 2$).

Other values of the constant C would merely scale the potential ϕ provided that the domain is the same.

Results for the straight jet are shown in Fig. 2 and for the expanding jet in Fig. 3. For $\beta < 10^{-2}$ the results are very close to the $\beta = 0$ or Poisson solution. Similarly, for $\beta > 10^2$ the curves are very close to the $\beta = \infty$ or Laplace solution. $\beta = 2.0$ represents a convenient intermediate case. Here, results start out close to the no-charge-depletion case but bend over toward the Laplacian due to the loss of charge. There is little difference between the straight jet and the expanding jet for $\beta = 2.0$ because the diverging portion happens where the charge has been substantially depleted. Moreover, for $\beta > 2.0$ no maxima appear.¹⁴ Figures 4–11 show equipotential and electric field maps of the cases considered as generated by the computer. The potential comes out of the solution to the equation. The electric field is the magnitude of the field normalized with the breakdown value; this feature of the program is useful because regions where the maximum electric field is exceeded are easily recognized.

V. CONCLUSIONS

The specific values of the parameters used here are representative of an electrogasdynamic generator.¹⁵ For example, $C = 23.146$ corresponds to an initial space-charge density of $1.03 \times 10^{-3} \text{ C/m}^3$, a length of 1 cm, and a V_0 of 5000 V. Also, $\beta = 2.0$ corresponds to the number density of oxygen at standard conditions

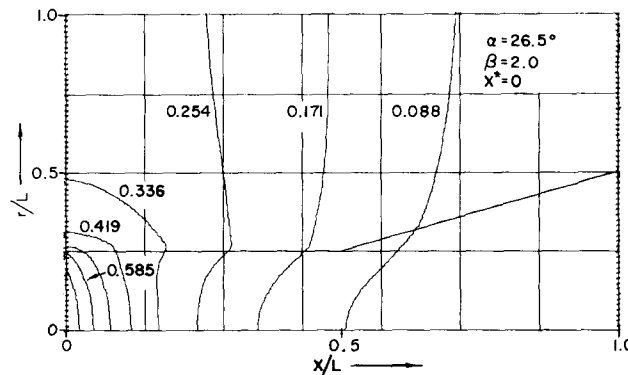


FIG. 11. Electric field map ($\alpha = 26.5^\circ, \beta = 2$).

($10^{25}/\text{m}^3$), a 10- μm spherical water droplet, and a Mach number of about 0.7 for the droplets (which is representative of the ratio v_p/\bar{c}). The maximum charge that a 10- μm droplet may have is 2×10^8 electrons and, as stated earlier, the attachment probability used was 10^{-7} (which is a conservative value).

The mobility of a 10- μm particle changed to the diffusion limit (corona charging¹⁵) is about $10^{-6} \text{ m}^2/\text{V sec}$, whereas ionic mobilities are above $10^{-4} \text{ m}^2/\text{V sec}$. These data are consistent with the assumptions fed into the calculations.

It may be concluded, therefore, that the charge depletion mechanism presented herein has a substantial influence in the performance of the EGD generator modeled. If anything, the fact that the space-charge density is reduced by a factor of 7.4 for the straight jet and for $\beta=2.0$ is significant (the output current would be reduced by the same amount). Moreover, in the application of voltage scheduling electrodes,¹⁶ for EGD generators, the distribution of the potential dictates where these electrodes are placed and charge depletion may have a significant effect in such a voltage distribution. It should also be mentioned that charge depletion acts the same way as charge spreading does in displacing the high-electric-field regions toward the injector plate.

The proposed mechanism for charge depletion could be checked experimentally by running a space-charge jet

into pure O_2 and then pure N_2 or argon under otherwise similar conditions and noting the effect on the over-all current.

*Lieutenant Commander, U.S. Navy, now at Moffett Field, Calif.

¹A. Marks, *J. Appl. Phys.* **43**, 219 (1972).

²O. Biblarz, *Energy Conversion* **10**, 207 (1970).

³J. D. Cobine, *Gaseous Conductors* (Dover, New York, 1958), Chap. 5.

⁴S. C. Brown, *Introduction to Electrical Discharges in Gases* (Wiley, New York, 1966), Chap. 7 and 8.

⁵B. D. Brier, *Proceedings of the International Conference of Cloud Physics*, Toronto, Canada, 1968 (unpublished).

⁶G. B. Wallis, *One-Dimensional Two-Phase Flow* (McGraw-Hill, New York, 1969), Chap. 12.

⁷R. N. Varney (private communication).

⁸L. E. Loeb (private communication).

⁹J. A. Decaire and M. O. Lawson, *Flight Symposium on MHD*, Stanford, Calif., 1967 (unpublished).

¹⁰L. B. Loeb, *Basic Processes of Gaseous Electronics* (U. C. Press, Berkeley, Calif., 1960), Chap. 5.

¹¹H. Schlichting, *Boundary Layer Theory*, 6th ed. (McGraw-Hill, New York, 1968), Chap. 24.

¹²C. M. Bohley, Aeronautical Engineer's thesis (Naval Postgraduate School, Monterey, 1972) (unpublished).

¹³J. E. Minardi, ARL Report No. 68-0156, 1968 (unpublished).

¹⁴It is interesting to note that the region of the maximum of the potential acts as a trough where the slower charged particles may get trapped and have a greater opportunity to lose their charge.

¹⁵O. Biblarz, K. E. Woehler, and T. H. Gawain, EGD Research Report No. NPS-57ZI0121A, 1970 (unpublished).

¹⁶M. Lawson and H. von Ohain, *J. Eng. Power* **93**, 201 (1971).